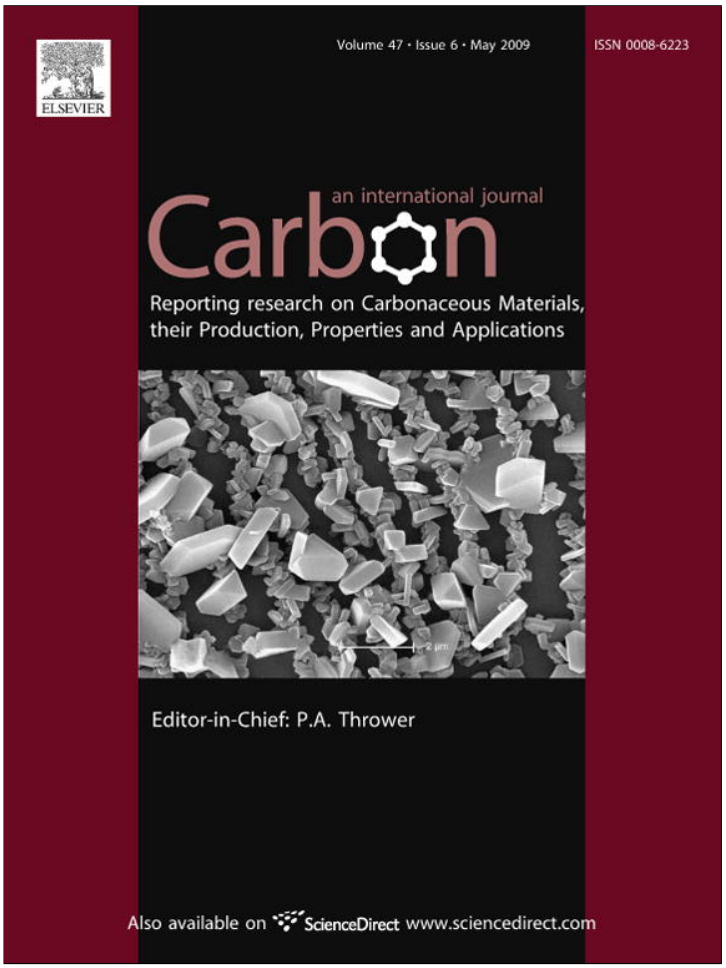

CARBON 47 (2009) 1501–1510

available at www.sciencedirect.com

ScienceDirect

journal homepage: www.elsevier.com/locate/carbon

Synthesis, characterization, and electrochemical testing of carbon nanotubes derivatized with azobenzene and anthraquinone

K. Sadowska[a], K.P. Roberts[b], R. Wiser[b], J.F. Biernat[a,*], E. Jabłonowska[c], R. Bilewicz[c]

[a]Department of Chemistry, Gdansk University of Technology, Narutowicza 11/12, 80-952 Gdansk, Poland
[b]Department of Chemistry and Biochemistry, The University of Tulsa, 800 S. Tucker Dr., Tulsa, OK 74104, USA
[c]Department of Chemistry, University of Warsaw, Pasteura 1, 02-093 Warsaw, Poland

ARTICLE INFO

Article history:
Received 27 October 2008
Accepted 26 January 2009
Available online 3 February 2009

ABSTRACT

Multi-walled and single-walled carbon nanotubes were side-wall functionalized with azobenzene and anthraquinone residues, i.e., chemical groups possessing redox activity, for potential utilization in functional catalysis and memory storage devices. Solvent-free synthesis was performed with diazonium salts generated in situ where it was found that it was simple and effective method. Nanotube functionalization was confirmed and characterized by Raman spectroscopy, X-ray photoelectron spectroscopy (XPS), and scanning electron microscopy (SEM). It is worth noting, that single-walled carbon nanotubes (SWCNTs) functionalized with azobenzene produced Raman modes typical of substituted azobenzenes with spectral peaks at ~1137, 1412, and 1447 cm^{-1}. The nanotubes containing electroactive substituents were transferred onto electrode substrates using the Langmuir–Blodgett approach and characterized by cyclic voltammetry. The amount of electroactive groups per mg of nanotubes was calculated based on the peak of cathodic current. A highly reproducible voltammetric response was obtained with a single nanotube layer or multiple nanotube/octadecanol layers. It is believed that devices such as these will be invaluable for future high-performance electrodes.

1. Introduction

Carbon nanotubes (CNTs), with their unique size, shape, and remarkable physical properties, are an extremely interesting allotropic form of carbon. As well, the electronic properties of single-walled carbon nanotubes (SWCNTs) are unique in that they can be either metallic or semiconducting, depending on their structure [1]. Most reports have shown that chemical modification of the nanotube side-wall or terminus is generally needed to control dispersion and assembly of CNTs into usable devices [2,3]. Although several synthetic routes for covalent modifications have been demonstrated, most require highly reactive carbenes, free radicals, or azomethine ylides [3]. We have previously reported that CNTs functionalized with azobenzene residues formed stable Langmuir and Langmuir–Blodgett monolayers [4,5]. As well, glassy-carbon electrodes (GCEs), modified with CNTs functionalized with anthraquinone residues were used in the process of catalytic reduction of oxygen in the presence of laccase [4,6].

In the current work, we describe a procedure for functionalization of SWCNTs and MWCNTs with redox active azobenzene and anthraquinone residues. The procedure based on coupling of free radicals generated from diazonium salts under solvent-free conditions produces materials of high level of modification. Multiple techniques were implemented in order to confirm functionalization, including Raman spectroscopy,

* *Corresponding author:* Fax: +48 58 347 1949.
E-mail address: biernat@chem.pg.gda.pl (J.F. Biernat).
0008-6223/$ - see front matter
doi:10.1016/j.carbon.2009.01.044

X-ray photoelectron spectroscopy (XPS), scanning electron microscopy (SEM) and cyclic voltammetry (CV). The novel CV application was determination of functionalization degree utilizing redox properties of bonded moieties. For this purpose the mono- and multilayers of CNTs were prepared with the use of the surfactant, octadecanol by Langmuir–Blodgett method. From the CV curves the amount of electroactive substituents was found out.

This approach to functionalization of CNTs leads to stable and reproducible modification of electrodes for applications in functional catalysis and memory devices.

Anthraquinone is known as catalyst in the reduction of oxygen and halogenated organics at electrodes or as mediator in heterogeneous biocatalysis, whereas azobenzene could play a role of photochemical switcher based on cis ⇄ trans isomerization. Immobilized mediators or molecular switches on CNTs do not leach to the solution, and when transferred onto electrode, they form stable nanostructured surfaces with catalytically or photochemically active centres. We expect that our approach will result in materials with novel properties, joining attributes of both, carbon nanotubes and attached residues. For heterogeneous biocatalysis, we anticipate that such approaches could increase the efficacy and reduce costs of catalytic processes.

2. Experimental

2.1. Materials and chemicals

Single-walled carbon nanotubes were purchased from CheapTubes.com, multi-walled carbon nanotubes were generously given to us by Nanoco Sp. z o.o. Zagorska St. 159, 42-600, Tarnowskie Góry, Poland. Distilled water was passed through a Milli-Q water purification system. All reagents and solvents were of analytical grade. The LiOH obtained from Merck, $HClO_4$ and citric acid from PPH POCH were used to prepare appropriate buffer solutions. Solutions were prepared daily.

2.2. Apparatus

Raman spectra were collected using a Witec confocal Raman microscope system (Ulm, Germany) equipped with a fiber-coupled Melles Griot (Carlsbad, CA) argon ion laser operating at 514.5 nm focused through a 60× objective. Collected light was dispersed through a triple monochromator (600 g/mm, 500 nm blaze angle) and detected with a thermoelectrically cooled (−60 °C) charge-coupled device. Sample preparation consisted of placing a small amount of carbon nanotubes in powder form between a microscope slide and a coverslip. Laser power at the sample was approximately 5 mW.

The XPS analyses were performed using ESCALAB MKII VG Scientific, (UK), spectrometer with base pressure in analytical chamber of $2{\cdot}10^{-9}$ mbar and non-monochromatized Mg Kα radiation (1253.6 eV). The spectra of elements were analyzed and de-convoluted into components described by an envelope of a Gaussian–Lorentzian sum function with an asymmetry tail. SEM images were taken on Leo 1530 microscope using 200–300 nm Au films deposited on borosilicate glass slides precoated with 1–4 nm underlayer of Cr (Arrandee).

Cyclic voltammetry experiments were conducted by using an Autolab potentiostat (ECO Chemie, Netherlands) in a three–electrode arrangement with a saturated calomel reference electrode, platinum foil counter electrode and an indium – tin oxide (ITO) working electrode. The ITO electrode was cleaned in hot acetone prior to experimentation.

2.3. Langmuir and Langmuir–Blodgett film formation

The curves of the surface pressure against the molecular area were recorded using the KSV LB trough 5000 equipped with hydrophobic barriers and controlled with KSV version 5000 software. A Wilhelmy balance was used as a surface pressure sensor. Surface pressure was recorded simultaneously as a function of molecular area. The accuracy of measurements was 0.01 nm^2 molecule for calculating area per molecule, and 1 mN/m^{-1} for surface pressure. The monocomponent monolayers or mixtures with octadecanol were transferred onto pre-cleaned indium – tin oxide (ITO) or evaporated gold on glass electrodes by withdrawing the substrates through the monolayer covered air–water interface at 20 mN/m surface pressure with a speed of 10 mm/min. After two hours of air-drying, the monolayer covered electrode was ready for use or for transfer of next layers.

2.4. Covalent functionalization of CNTs

Nanotubes functionalized with azobenzene (AZOB) and anthraquinone (AQ), as illustrated in Fig. 1, were obtained by adaptation of methods previously described [7].

Briefly, 50 mg (~4 mmol of carbon) of SWCNTs or MWCNTs were mixed with an adequate amount of amine i.e., 2-aminoanthraquinone (MW 223 g/mol), or *p*-aminoazobenzene (MW 197 g/mol). The amount of amine was 4 equivalents per mole of total CNT carbon. After the mixture was placed in a round-bottomed flask equipped with a magnetic stir bar, isoamyl nitrite (4.8 equiv per mole of carbon; MW 117 g/mol), prepared as described in [8], was added. The resultant paste was heated to 75 °C to generate free radicals, and stirred under argon for 24 h. Then, the reaction mixture was diluted with DMF and centrifuged. The collected solid was washed extensively with DMF, next with anhydrous THF and dried under reduced pressure.

3. Results and discussion

3.1. Characterization of derivatized SWCNTs

Initial characterization of pristine SWCNTs was conducted using SEM imaging as shown in Fig. 2. SWCNTs were found as bundles of long tubes. Estimated diameters are less than 1.5 nm. Traces of amorphous carbon were visible.

Derivatized SWCNTs were also tested by Raman spectroscopy. The distinctive Raman modes of CNTs are primarily due to confinement of electronic and phonon states. Several excellent reviews have been written regarding Raman spectroscopy of SWCNTs [9–11]. Of the several vibrational modes

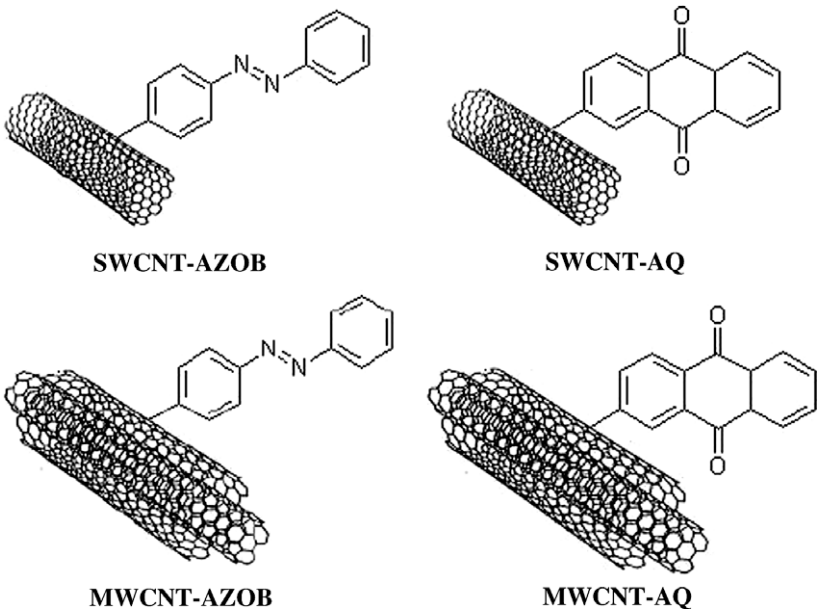

Fig. 1 – Schematic presentation of functionalized carbon nanotubes.

and overtones observed in our Raman results for pristine and functionalized SWCNTs, four primary Raman modes were monitored: (i) the radial breathing motion (RBM) modes, (ii) the disorder *D* band, (iii) the graphite *G* band, and (iv) the overtone *G′* band. Example Raman spectra are shown in Fig. 3 for pristine SWCNT starting material (a), SWNCTs derivatized with anthraquinone (AQ) (b), and SWCNTs derivatized with azobenzene (AZOB) (c). All spectra were normalized to the tangential *G* band at ~1584–1588 cm^{-1} in the spectra.

The first-order RBM modes ($\omega_{RBM} < 300\ cm^{-1}$) are unique to SWCNTs and correspond to symmetric in-phase displacements of carbon atoms in the radial direction. Although not completely quantitative, the intensity, position, and spectral width of RBM modes have been correlated to various factors such as nanotube size, metallic/semiconductor ratio, (*n*,*m*) assignments, and charge transfer to substituents on the nanotube surface [10]. As shown in Fig. 4, substantial reduction in the intensity of the lower frequency RBM modes was observed for AQ- or AZOB-derivatized SWCNTs as compared to the pristine starting material. As well spectral shifts and broadening were observed. Similar results were reported by Fantini et al., where spectral shifts, broadening, and reduction in RBM intensity were attributed to displacement of the Fermi level due to the added functional group on the CNT side-wall [12]. As well, the authors postulated that fluctuations in the intensity of the RBM modes indicate differential functionalization of semiconducting versus metallic SWCNTs.

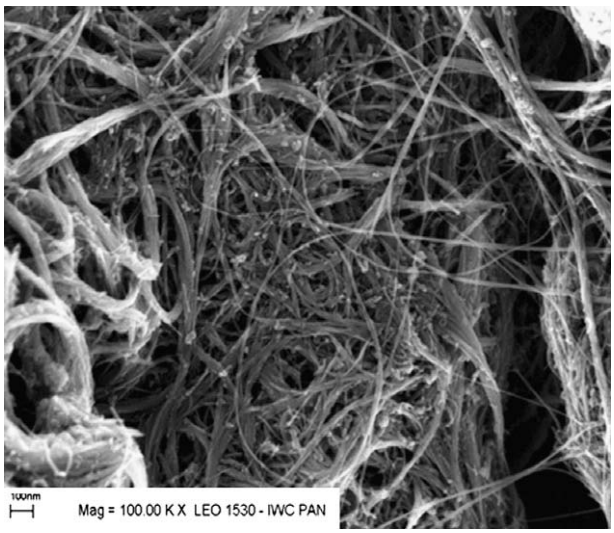

Fig. 2 – SEM images of pristine single-walled carbon nanotubes.

Although the intensity of the RBM modes for AQ and AZOB functionalized SWCNTs both decreased relative to pristine SWCNTs, only AQ-derivatized SWCNTs produced a significant spectral shift. As shown in the normalized spectrum of AQ-SWCNTs in Fig. 4, the primary RBM mode in the metallic region shifted from 269 to 380 cm^{-1}. This is strong indication of side-wall functionalization and disruption of the radial breathing motion due to the added functionality. Moreover, after extensive purification, the resultant AQ-SWCNT product appears to be largely composed of small semiconductor nanotubes SWCNTs as evidenced by RBM modes at 172 and 207 cm^{-1} (~1.2–1.4 nm). Similar results have been previously reported [13].

For AZOB-SWCNTs (spectrum c), spectral shifts and relative intensity changes of the RBM modes showed a less drastic difference when compared to pristine SWCNTs. Unlike derivatization with AQ, AZOB appears to have a similar reactivity toward both metallic and semiconducting tubes with a relative intensity distribution about the same as the starting material. Inversion of the ratio of the 172 and 207 cm^{-1} mode intensities suggests a slightly preferential labeling of one type of semiconductor tube over another. The assignment of the various types of nanotubes possible is beyond the scope of

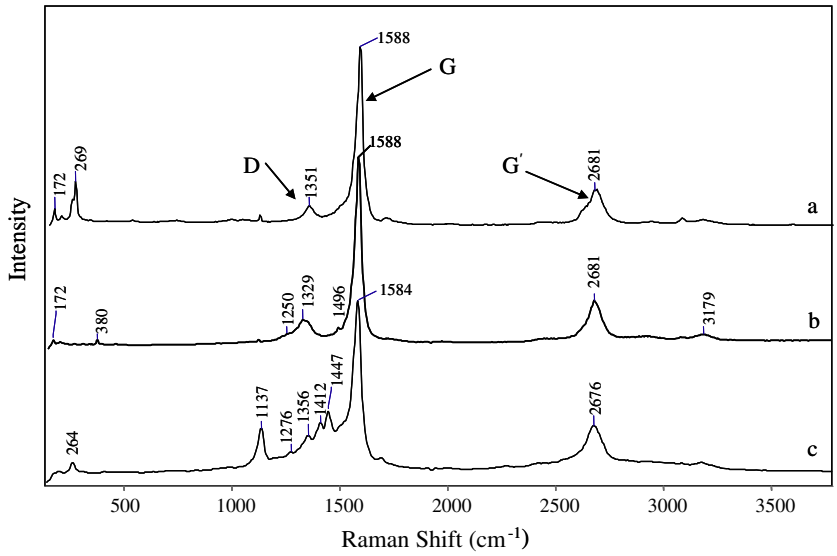

Fig. 3 – Comparison of Raman spectrum of pristine and functionalized SWCNTs. Spectra a–c correspond to pristine SWCNTs, SWCNT-AQ, SWCNT-AZOB.

what is presented here and is the subject of future investigations. Nonetheless, by comparing the RBM modes of pristine versus AQ- and AZOB-derivatized products, it can be concluded that covalent side-wall attachment was successful in both cases.

The disorder *D* band in SWCNTs is observed when the symmetry of hexagonal sp^2 bonded lattice is disrupted due to, for example, covalent side-wall functionalization [10,12].

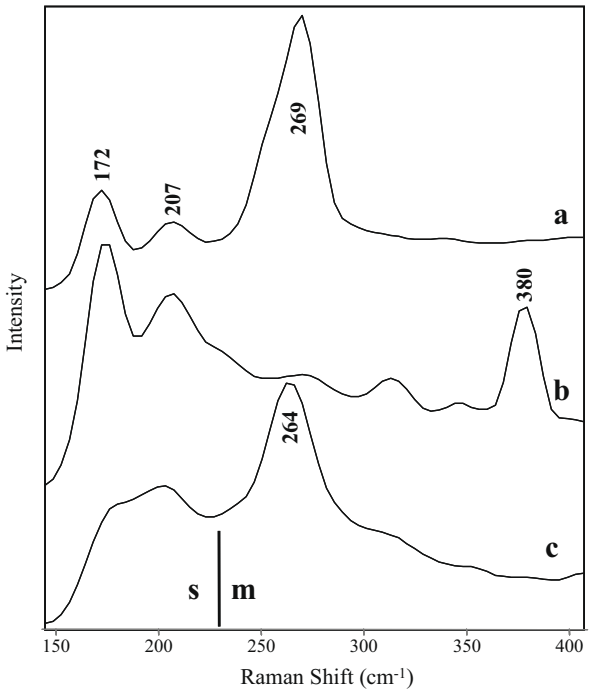

Fig. 4 – Normalized RBM Raman modes for pristine SWCNTs (a), AQ-derivatized SWCNTs (b), and AZOB-derivatized SWCNTs (c). The line at approximately 225 cm^{-1} separates semiconducting versus metallic vibration modes.

As shown in the spectra of Fig. 3a, the weak *D* mode present at ~1350 cm^{-1} for pristine SWCNTs implies high sample purity. RBM modes were observed from ~170–270 cm^{-1}, indicative of the diversity of diameters within the nanotube population. The *G* mode at ~1588 cm^{-1} and the *G′* mode at ~2680 cm^{-1} are also consistent with reported values for pristine SWCNTs [9]. On the other hand, there is considerable divergence in the *D* band region for AZOB-SWCNTs (spectrum c), while less change in the *D* band for AQ-SWCNTs (spectrum b). Even after exhaustive purification (see Experimental), the Raman spectrum of AZOB-SWCNTs (Fig. 3c), produced several unique modes indicative of azobenzene functionality; a symmetric C–N stretching mode (1137 cm^{-1}), the N=N stretching mode (1412 cm^{-1}), and a combination of N=N and phenyl ring modes at 1447 cm^{-1}. Generally, the degree of functionalization is such that the intensity of the Raman modes for the functional group moiety are buried beneath the nanotube Raman modes. Thus, the presence of resolvable AZOB Raman modes suggests a large degree of functionalization by azobenzene using in situ derivatization.

Derivatization with AQ produced less clear evidence of functionalization when monitoring the *D* band as shown in spectrum b of Fig. 3. The *D* band, although small, broadened as compared to pristine nanotubes with an additional component at ~1250 cm^{-1}. Although tentative, the new component in the Raman spectrum could be from C–C vibrations of anthraquinone.

Further confirmation of side-wall functionalization was provided by measuring the relative integrated intensity ratio of the one phonon double-resonance *D* band to the first-order tangential *G* band, i.e., the I_D/I_G ratio. The tangential *G* band is primarily a convolution of C–C vibrations along the nanotube axis (G^+) while the lower frequency mode (G^-) is attributed to vibrations along the nanotube circumference. The former has been shown to be sensitive to SWCNT surface modification and the latter as a useful indicator of metallic versus semiconductor nanotubes [10,12,13]. The integrated intensity of

the *D* band increased strongly (Fig. 3) as compared to the pristine nanotubes with I_D/I_G ratios of 0.12, 0.26, 0.67 for pristine, AQ-, and AZOB-SWCNTs, respectively. The peak is not observed to increase as a result of adsorption of, for example, hydronium ions or surfactants on the nanotube side-walls, thus it allows for distinguishing covalent from non-covalent modification. For AQ-, and AZOB-SWCNT samples, the average RBM mode intensity with the reference to the *G* mode decreased; as compared to the pristine SWCNTs. Normalized RBM Raman modes for pristine and modified SWCNT are presented in Fig. 4.

Our results for SWCNT in situ functionalization are generally in agreement with the electrochemical reduction of aryl diazonium salts grafted to SWCNTs in terms of relative fluctuations of RBM modes and an increased I_D/I_G ratio upon functionalization. However, Bahr et al. did not observe such stark changes in the intensities of RBM modes, *D* and *G* bands, for SWCNTs functionalized by electrochemical reduction reactions of aryl diazonium salts [14]. It was reported that, although significant spectral shift was observed, the intensity of the disorder mode increased upon functionalization. The intensity of the tangential *G* mode was also increased relatively to that of the radial breathing mode in most cases, and the overall intensity was lower. Our results are in agreement with these, although we observed Raman modes specific for the binding moiety. This suggests either a higher degree of nanotube functionalization or possible Raman enhancement effects of the binding moiety on the nanotube backbone. Dyke and Tour used *p*-substituted aromatic diazonium salts generated in situ to introduce a variety of functional groups onto the SWCNT side-walls [7]. They applied several techniques, including Raman spectroscopy, to ensure that the nanotube side-wall is changed through covalent bond formation. The Raman spectra obtained for nanotubes modified by their method is similar to our spectra, so that the RBM (230 cm^{-1}) and *G* modes (1590 cm^{-1}) characteristic for SWCNTs are present, but the *D* mode (1290 cm^{-1}) is greatly enhanced.

Although the two-phonon *G′* band has been shown to be relatively insensitive to functionalization [10], a comparison of pristine to derivatized SWCNTs can provide important information about the type of nanotube starting material and reaction products. The double-resonance *G′* mode originates as the second harmonic of the disorder-induced *D* band in graphite. In SWCNTs, the *G′* band can either be a single Lorentzian peak (as in graphite and MWCNTs) or as a bimodal peak with distinct origins for semiconducting and metallic SWCNTs. In semiconducting SWCNTs, the splitting of the *G′* band is attributed to phonon dispersion in opposite directions to the anisotropic phonon dispersion in metallic nanotubes.

As shown in Fig. 3a, the *G′* band is bimodal in the case of pristine SWCNTs, suggesting a mixture of several types of SWCNTs in the starting material. However, after reaction with anthraquinone (Fig. 3b) and azobenzene (Fig. 3c), the resultant *G′* mode Raman bands are mainly single-mode peaks with a slight blue-shift ($\Delta\omega \sim 5$ cm^{-1}) for AZOB-SWCNTs. This suggests that the nanotubes were activated by the in situ process and provides additional evidence of a preferential binding of the electroactive substituents to specific type(s) of nanotubes. However, it can not be ruled out that the loss of the bimodal *G′* band could be due to differences in sample reaction processing and purification conditions to those of the pristine control.

3.2. *Characterization of derivatized MWCNTs*

Initial characterization of pristine MWCNTs was carried out using SEM imaging as shown in Fig. 5. They exist in flakes, made of twisted nanotubes, with diameters between 20–50 nm.

Raman spectroscopy was also utilized to characterize in situ functionalization of MWCNTs with AQ and AZOB. Like single-walled tubes, MWCNTs exhibit strong quantum confinement effects that allow for resonance enhancement of the graphite *G* Raman mode and the dispersive *D* mode. However, unlike SWCNT spectra, the RBM modes are too weak to be observed for the larger diameter multi-walled tubes. As well, the dispersive *D′* bands are seen in MWCNTs but not SWCNTs. The dispersive *D* band is much more prominent in MWCNT Raman spectra due to large distribution of the density of states in multi-walled systems. It has been shown that spectral shifts of *G* and *D* Raman modes can be used to indicate side-wall or end-cap functionalization [11]. However, the degree of spectral shift was shown to be more dependent on the electron donating/accepting nature of the substituent than the degree of functionalization. In addition, several second-order bands such as the *G′* band are commonly observed in MWCNT Raman spectra and have also been considered as potentially useful for characterization of carbon nanotubes upon chemical or physical modification [15]. Although complete quantitative interpretation has yet to be developed for the intensities of the first- and second-order Raman processes, it has clearly been shown to be a useful tool for MWCNT investigations, especially when coupled with physical property data and results from various microscopy and spectroscopy techniques.

Commonly, the relative intensity ratios of *D* to *G* bands (I_D/I_G) are utilized as an approach to monitoring the purity

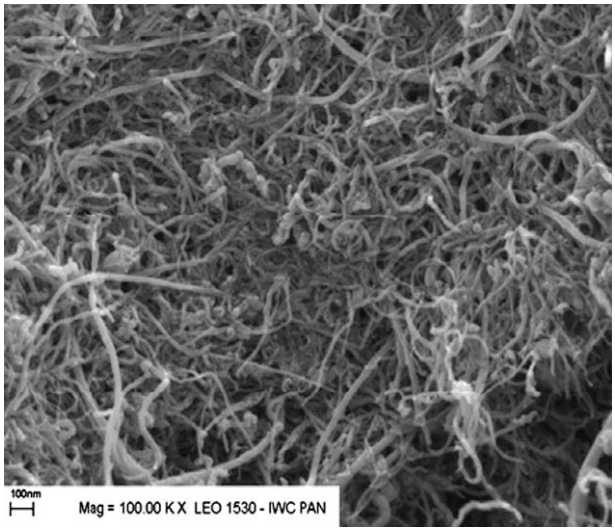

Fig. 5 – SEM images of pristine multi-walled carbon nanotubes.

and functionalization of MWCNTs. An increase in the *D* band intensity (I_D) has been shown to be an indication of side-wall $sp^2 \rightarrow sp^3$ hybridization from covalent binding of functional various moieties [9,16–18]. However, it has also been demonstrated that the direct I_D/I_G relationship can be misleading due to the dependence of the intensities on several experimental factors such as laser excitation frequency, laser intensity, samples preparation conditions, and atmospheric conditions. As well, it has been reported that functionalizing nanotubes can effectively produce smaller length nanographitic crystallinity that could offset defect-site contributions to the *D* band intensity in the Raman spectrum [12]. Further evidence suggested that the relationship of I_D/I_G was more accurate if the intensities were measured relative to the intensity of the second-order *G*′ band ($I_{G'}$) [15]. It was proposed that the two-phonon *G*′ mode intensity decreases as the uniformity in the sample decreases due to the presence of impurities and/or a large distribution of nanotube types and sizes. In either case, nanotube coupling is disrupted which could result in decreased two-phonon *G*′ band intensity. However, other reports have indicated that such a direct correlation is not well understood [19].

Reports have also shown that Raman intensity ratios relative to *D*′ bands (~1585 cm^{-1}) can provide evidence of nanotube modification and purity [9,16–18]. The dispersive *D*′ mode originates from vibrations perpendicular to the nanotube walls and is related to the strongly dispersive *D* mode where *D*′ is nearer to the *Γ* point and *D* nearer the *K* point in the Brilouin zone in graphite [20,21]. Here we report the relative intensity contributions and bandwidths of *D*, *G*, *D*′, and *G*′ Raman modes for pristine and functionalized MWCNTs (Table 1). Raman modes of lower intensity were not characterized.

Shown in Fig. 6 are typical Raman results for pristine MWCNTs (spectrum a), MWCNTs functionalized with AQ (b) and AZOB (c). Inset is an example of *D*′ and *G* peak fitting using Gaussian and Lorentzian fitting, respectively, for pristine MWCNTs. Integrated intensities were used for determining the relative contributions from each Raman mode. As seen in the figure, *D*, *G*, *D*′ and *G*′ bands are present at expected frequencies at ~1358, 1592, 1620, and 2710 cm^{-1}. However, the I_D/I_G ratio (Table 2) unexpectedly decreased for AQ- and AZOB-functionalized MWCNTs. The intense *D* mode is observed when the symmetry of the hexagonal sp^2 bonded

Table 1 – Observed Raman modes for pristine and functionalized MWCNTs.

	D band	*G* band	*D*′ band	*G*′ band
	Position (fwhm) (cm^{-1})	Position (fwhm) (cm^{-1})	Position (fwhm) (cm^{-1})	Position (fwhm) (cm^{-1})
Pristine MWCNTs	1358 (54.8)	1592 (50.6)	1626 (24.3)	2710 (84.5)
AQ-MWCNTs	1352 (53.6)	1582 (42.7)	1614 (30.3)	2699 (69.9)
AZOB-MWCNTs	1358 (49.4)	1585 (36.8)	1624 (26.5)	2706 (62.0)

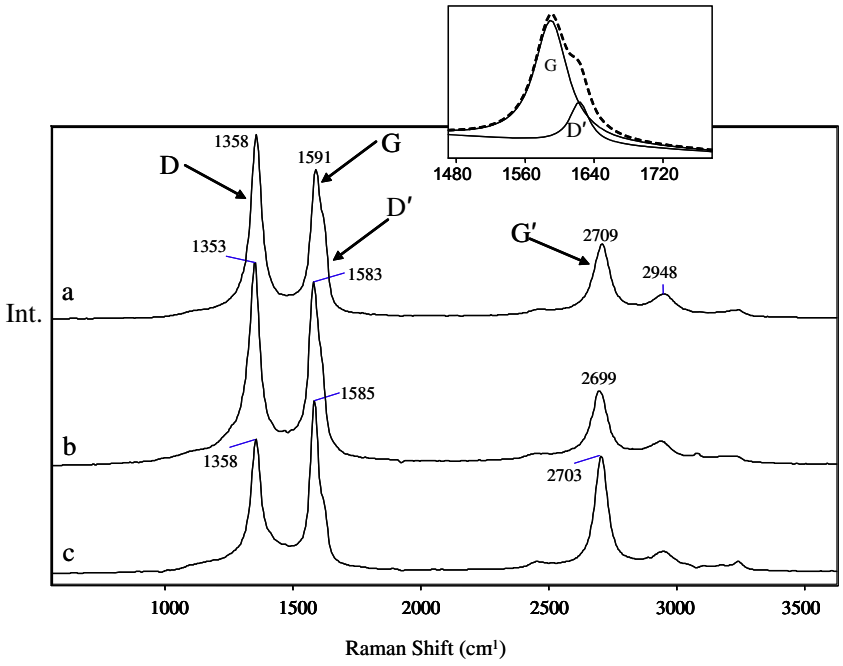

Fig. 6 – Raman spectra of pristine and functionalized MWCNTs. Spectrum a is for pristine SWCNT starting material, spectrum b is for SWCNT-AQ and spectrum c is for SWCNT-AZOB. Inset is an example peak fitting for the relative contributions from *D*′ and *G*.

Table 2 – Ratios of modes intensities for pristine and modified MWCNT.

	D/G	G′/D	G′/G	D′/D	G′/D′
Pristine MWCNTs	1.36	0.60	0.81	0.06	9.30
AQ-MWCNTs	1.40	0.43	0.60	0.08	5.12
AZOB-MWCNTs	1.03	1.12	1.15	0.11	9.97

lattice is disrupted, so it may determine the covalent functionalization, but may also be due to the presence of amorphous carbon in the tested sample. The latter is probable in our case since the starting material was not able to be subjected to identical processing and reaction conditions to that of the AQ- and AZOB-MWCNT products. This can also be observed by monitoring the width of the Raman bands. As shown in Table 2, the full-width at half-maximum decreases upon functionalization, indicating a more narrow distribution of nanotubes as compared to the starting material.

Similar results were reported by Bacsa et al. [22] for MWCNTs with diameters ranging between 8–30 nm. As well, Raman spectra for MWCNTs with larger diameters, as examined by Chandrabhas et al. (15–50 nm) [23], and Kastner et al. (20–80 nm) [24] are very similar to disordered graphite. More recently, DiLeo et al. [15] demonstrated the use of the *D*, *G*, and *G*′ Raman bands to assess the purity of MWCNTs. It was proposed that the $I_{G'}/I_D$ ratio was the most sensitive to side-wall functionalization, where an exponential calibration curve was derived. Our results, however, indicate that the $I_{D'}/I_D$ intensity ratio provides the greatest difference (sensitivity) between functionalized and pristine MWCNTs.

Further confirmation of AZOB-functionalization was accomplished through XPS measurement of AZOB-MWCNT. The nanotube samples were blended with melted polyethylene and thin films were formed, which were mounted on the spectrometer probe tip. Wide scan spectra in the binding energy range 0–700 eV were obtained (Fig. 7a). The XPS spectrum shows distinct carbon and nitrogen peaks. Fig. 7b shows narrow scan spectra of the C 1s region of the MWCNT-AZOB. The binding energy equal to 285.0 eV, corresponds to sp^2 and sp^3 hybridized carbon atoms. Fig. 7c shows narrow scan spectra of the N 1s region. The binding energy 398.6 eV refers to the azo bond [25].

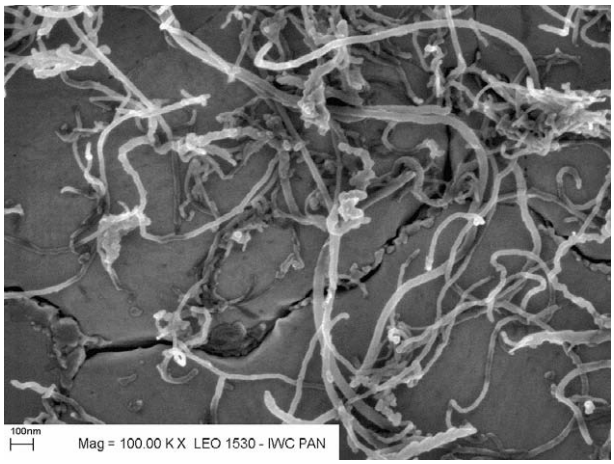

Fig. 8 – SEM image of mixed monolayer of AZOB-MWCNT: octadecanol 3:1 (w/w) evaporated on a gold electrode.

3.3. *Langmuir–Blodgett films of SWCNT-AZOB and MWCNT-AZOB*

Functionalized with azobenzene moieties, SWCNT-AZOB and MWCNT-AZOB were found to form stable Langmuir and Langmuir–Blodgett monolayers. In order to utilize the CNTs for the formation of nanostructured substrates, the nanotubes have to form reproducible films. The procedure involving the Lang-

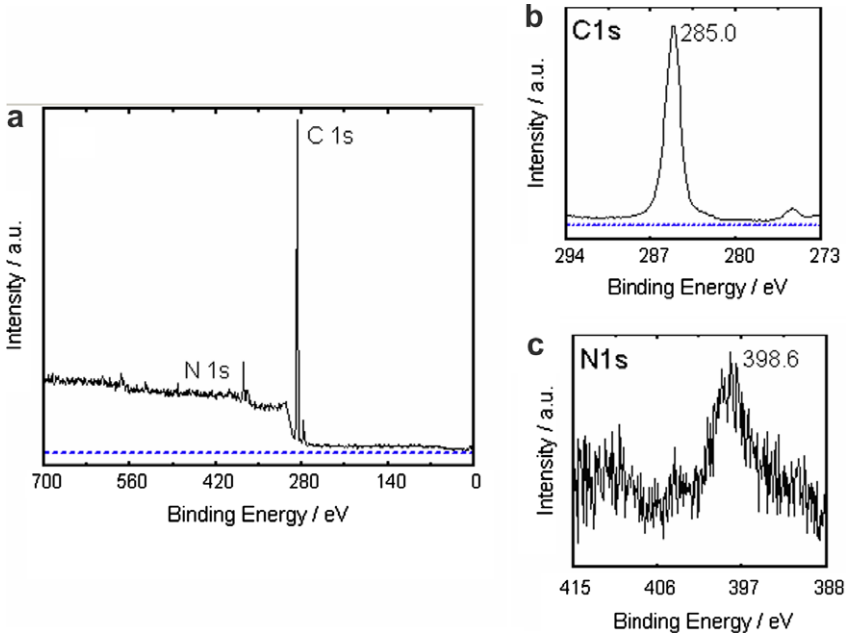

Fig. 7 – XPS spectrum of MWCNT-AZOB (a) wide scan spectrum; (b) C 1s narrow scan spectrum; (c) N 1s narrow scan spectrum.

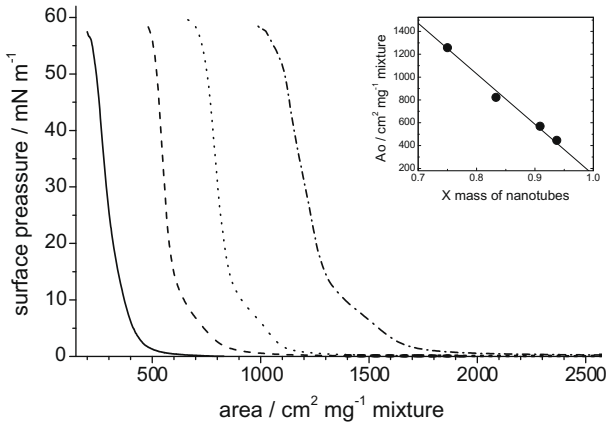

Fig. 9 – Isotherms of surface pressure – area per mg of the solutes. Mass fraction of nanotubes: (solid line) – 0.9375, (dashed) – 0.9090, (dot) 0.8333, (dashed line) 0.7500.

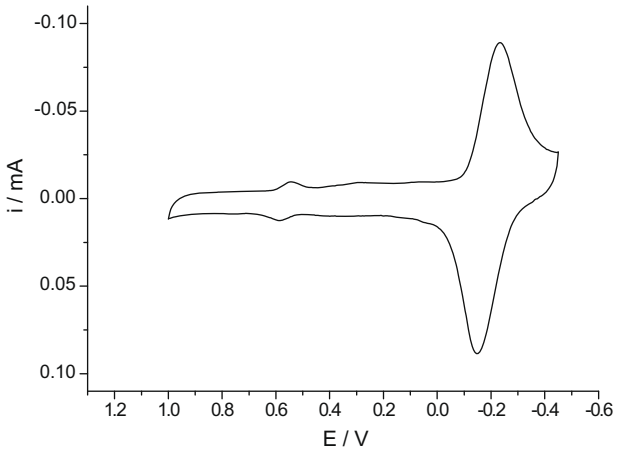

Fig. 11 – Cyclic voltammogram recorded in 0.1 M H_2SO_4 solution for MWCNT-AQ: octadecanol mixed monolayer (10:1 w/w), transferred onto ITO electrode, υ = 100 mV/s.

muir–Blodgett technique allows for the preparation of well organized films and for transfer on solid surfaces. In the case of nanotubes, mixed films have to be prepared with a surfactant playing the role of matrix and monolayer "diluent". The nanotube component spans the monolayer in the form of a network. The surfactant decreases the unfavorable aggregation of nanotubes and allows stable attachment of the film to the electrode. The SEM image (Fig. 8) reveals uniform coverage of the electrode by the octadecanol monolayer spanned with the network of SWCNT-AZOB since underlying terraces of the gold substrate can be clearly recognized.

Modified SWCNT-AZOB dispersed in chloroform solution of octadecanol was spread on the water surface and compressed with a surface pressure of 60 mN/m before the collapse of the organized layer. The isotherms for SWCNT-AZOB – octadecanol mixed films are shown for different ratios of components in chloroform solution (Fig. 9).

The nanotubes were transferred onto solid substrates of Au or ITO using the Langmuir–Blodgett approach at 20 mN/m. Cyclic voltammograms recorded for electrodes modified by SWCNT-AZOB : octadecanol films (10:1 mass ratio) are presented in Fig. 10.

Since azocompounds are electroactive, the surface concentration of the compound present on the conducting support can be evaluated based on the charge of the voltammetric reduction peak:

$$\Gamma = \left(\frac{Q}{nFA}\right) \quad (1)$$

where Γ (mol/cm^2) – surface concentration of the electroactive component, Q (C) – charge under cathodic peak, n – number of electrons exchanged, A[cm^2]–working area of the electrode.

The charge and current increase proportionally to the number of layers transferred from the air water interface. Based on surface concentration measurements, for each monolayer, the extent of nanotube modification can be calculated and the value determined to be 3.7×10^{-8} moles of azobenzene per 1 mg of nanotubes.

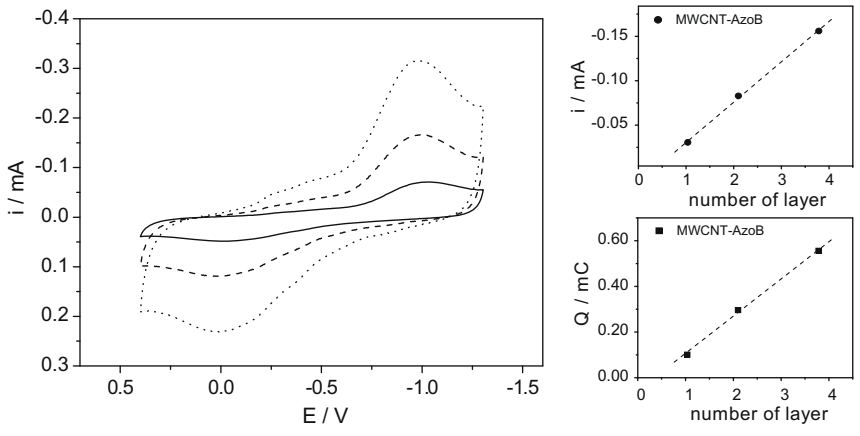

Fig. 10 – Cyclic voltammograms recorded in 1 M $LiClO_4$ + NaOH 0.02 M, pH 12 using) at 100 mV/s electrodes modified by MWCNT-AZOB : octadecanol films (10:1 mass ratio. Insets: Current and charge of the reduction peak vs. number of layers transferred.

For the single-walled nanotubes modified with anthraquinone the voltammograms obtained in acidified solutions show the peaks are even more reversible (Fig. 11). Reversible reduction/oxidation peaks at ca. −0.2 V correspond to hydroquinone formation/oxidation at the electrode. Based on the charge of the peak the extent of nanotube modification can be evaluated as 7.0×10^{-8} moles of anthraquinone per 1 mg of nanotubes.

Banks et al. [6] reported derivatization of multi-walled carbon nanotubes via the reduction of anthraquinone-1- diazonium chloride with hypophosphorous acid. For this nanomaterial, with covalently attached anthraquinone, electrocatalytic activity was explored. They modified basal plane pyrolytic graphite electrodes with chemically modified MWCNTs, and found the surface coverage of the immobilized anthraquinone to be 2.04×10^{-10} mol/cm^2. The surface concentration of anthraquinone in our case using SWCNTs is similar and equal to $3.6 \pm 0.9 \times 10^{-10}$ mol/cm^2.

4. Conclusions

Syntheses of SWCNTs and MWCNTs with chemically bonded redox active residues of azobenzene and antraquinone were successfully achieved using coupling of respective radicals generated from aminoazobenzene and aminoanthraquinone upon treatment with isoamyl nitrite. Their structures were proven by several electrochemical and spectroscopic methods. It was also shown that the derivatized CNTs form mixed monolayers with octadecanol on water subphases, which, in turn, can be transferred onto solid conducting substrates and studied by electrochemical methods.

It was found, that the integration of the voltammetric response from the electroactive substituents on the nanotube surface can provide a measure of the degree of functionalization. The high reproducibility of the elaborated procedures for electrode modification with networks of nanotubes possessing electroactive substituents makes it promising for the preparation of surfaces for electrocatalysis and memory devices and work in these directions is underway in our laboratories.

Acknowledgements

Financial support of this work by the Polish Ministry of Sciences and Higher Education, Grants Nr. GDRE/18/2007-PS18 and Nr. N N204 223834 is kindly acknowledged. This work was also supported by the US Air Force Research Laboratory and Air Force Office of Scientific Research under grant number FA9550-06-1-0365. In addition, the authors thank the Office of Research at the University of Tulsa for their support of this research. We would also like to acknowledge NSF-Oklahoma EPSCoR for their support.

REFERENCES

[1] Rakov EG. Gogotsi Y, editor. Nanomaterials handbook. Boca Raton: CRC Press; 2006.

[2] Mitchell CA, Bahr JL, Arepalli S, Tour JM, Krishnamoorti R. Dispersion of functionalized carbon nanotubes in polystyrene. Macromolecules 2002;35(23):8825–30.

[3] Banerjee S, Hemraj-Benny T, Wong S. Covalent surface chemistry of single-walled carbon nanotubes. Adv Mater 2005;17(1):17–29.

[4] Sadowska K, Jabłonowska E, Stolarczyk K, Wiser R, Bilewicz R, Roberts KP, et al. Chemically modified carbon nanotubes: synthesis and implementation. Polym J Chem 2008;82:1309–13.

[5] Nazaruk E, Sadowska K, Madrak K, Biernat J, Rogalski J, Bilewicz R. Composite bioelectrodes based on lipidic cubic phase with carbon nanotube network. Electroanalysis. doi:10.1002/elan.200804435.

[6] Banks CE, Wildgoose GG, Heald CGR, Compton RG. Oxygen reduction catalysis at anthraquinone centres molecularly wired via carbon nanotubes. J Iran Chem Soc 2005;2(1):60–4.

[7] Dyke ChA, Tour JM. Solvent-free functionalization of carbon nanotubes. J Am Chem Soc 2003;125(5):1156–7.

[8] Canning PS, McCrudden K, Maskill H, Sexton B. Rates and mechanisms of the thermal solvolytic decomposition of arenediazonium ions. J Chem Soc Perkin Trans 2 1999;12:2735–40.

[9] Dresselhaus MS, Dresselhaus G, Saito R, Jorio A. Raman spectroscopy of carbon nanotubes. Phys Rep 2005;409(2):47–99.

[10] Dresselhaus MS, Dresselhaus G, Jorio A. Raman spectroscopy of carbon nanotubes in 1997 and 2007. J Phys Chem C 2007;111(48):17887–93.

[11] Lefrant S, Baibarac M, Baltog I, Buisson JP, Chauvet O. Raman and SERS studies of carbon nanotubes. Mol Cryst Liq Cryst 2002;374(1):325–34.

[12] Fantini C, Usrey ML, Strano MS. Investigation of electronic and vibrational properties of single-walled carbon nanotubes functionalized with diazonium salts. J Phys Chem C 2007;111(48):17941–6.

[13] Liu J, Dossot M, Olevik D, Mamane V, Vigolo B, Abrahamsson D, et al. Preferential functionalisation of carbon nanotubes probed by Raman spectroscopy. Physica E 2008;40(7):2343–6.

[14] Bahr JL, Yang J, Kosynkin DV, Bronikowski MJ, Smalley RE, Tour JM. Functionalization of carbon nanotubes by electrochemical reduction of aryl diazonium salts: a bulky paper electrode. J Am Chem Soc 2001;123(27):6536–42.

[15] DiLeo RA, Landi BJ, Raffaelle RP. Purity assessment of multiwalled carbon nanotubes by Raman spectroscopy. J Appl Phys 2007;101(6):064307–0643012.

[16] Osswald S, Flahaut E, Ye H, Gogotsi Y. Elimination of D-band in Raman Spectra of double-wall carbon nanotubes by oxidation. Chem Phys Lett 2005;402(4–6):422–7.

[17] Osswald S, Flahaut E, Gogotsi Y. In situ Raman spectroscopy study of oxidation of double- and single-wall carbon nanotubes. Chem Mater 2006;18(6):1525–33.

[18] Osswald S, Havel M, Gogotsi Y. Monitoring oxidation of multiwalled carbon nanotubes by Raman spectroscopy. J Raman Spectrosc 2007;38(6):728–36.

[19] Antunes EF, Lobo AO, Corat EJ, Trava-Airoldi V-J, Martin AA, Veríssimo C. Comparative study of first- and second-order Raman spectra of MWCNT at visible and infrared laser excitation. Carbon 2006;44(11):2202–11.

[20] Grüneis A, Saito R, Kimura T, Cançado LG, Pimenta MA, Jorio A, et al. Determination of two-dimensional phonon dispersion relation of graphite by Raman spectroscopy. Phys Rev B 2002;65(15):155405–7.

[21] Saito R, Jorio A, Souza Filho AG, Dresselhaus G, Dresselhaus MS, Pimenta MA. Probing phonon dispersion relations of graphite by double resonance Raman scattering. Phys Rev Lett 2002;88(2):027401-1–4.

[22] Bacsa WS, Chatelain DUA, de Heer WA. High-resolution electron microscopy and inelastic light scattering of purified multishelled carbon nanotubes. Phys Rev B 1994;50(20):15473–6.
[23] Chandrabhas N, Sood AK, Sundararaman D, Raju S, Raghunathan VS, Rao GVN, et al. Structure and vibrational properties of carbon tubules. Pramana J Phys 1994;42(5):375–85.
[24] Kastner J, Pichler T, Kuzmany H, Curran S, Blau W, Weldon DN, et al. Resonance Raman and infrared spectroscopy of carbon nanotubes. Chem Phys Lett 1994;221(1–2):53–8.
[25] Nakayama Y, Takahagi T, Soeda F, Ishitani A, Shimomura M, Kunitake T. XPS study of oriented organic molecules. Vesicles of azobenzene-containing alkyl ammonium amphiphiles. J Colloid Interf Sci 1988;122(2):464–74.